PHILOSOPHICAL TRANSACTIONS B

royalsocietypublishing.org/journal/rstb

Research

Cite this article: Zhang W *et al*. 2019 Enhancement of oxidative stress contributes to increased pathogenicity of the invasive pine wood nematode. *Phil. Trans. R. Soc. B* **374**: 20180323.
http://dx.doi.org/10.1098/rstb.2018.0323

Accepted: 16 October 2018

One contribution of 19 to a theme issue 'Biotic signalling sheds light on smart pest management'.

Subject Areas:
ecology, evolution

Keywords:
Bursaphelenchus xylophilus, fecundity, pathogenicity, reactive oxygen species, manganese superoxide dismutase

Authors for correspondence:
Jianghua Sun
e-mail: sunjh@ioz.ac.cn
Zhen Zou
e-mail: zouzhen@ioz.ac.cn

†These authors contributed equally to this work.

Electronic supplementary material is available online at https://dx.doi.org/10.6084/m9.figshare.c.4325879.

THE ROYAL SOCIETY PUBLISHING

Enhancement of oxidative stress contributes to increased pathogenicity of the invasive pine wood nematode

Wei Zhang[1,3,†], Lilin Zhao[1,4,†], Jiao Zhou[1], Haiying Yu[2], Chi Zhang[1,4], Yunxue Lv[1,4], Zhe Lin[1], Songnian Hu[2], Zhen Zou[1,4,5] and Jianghua Sun[1,4]

[1]State Key Laboratory of Integrated Management of Pest Insects and Rodents, Institute of Zoology, and [2]CAS Key Laboratory of Genome Sciences and Information, Beijing Institute of Genomics, Chinese Academy of Sciences, Beijing 100101, People's Republic of China
[3]Laboratory of Forest Pathogen Integrated Biology, Research Institute of Forestry New Technology, Chinese Academy of Forestry, Beijing 100091, People's Republic of China
[4]College of Life Science, University of Chinese Academy of Sciences, Beijing 100049, People's Republic of China
[5]School of Medicine, Huzhou University, Huzhou 311300, People's Republic of China

JS, 0000-0002-9465-3672

Reactive oxygen species (ROS) play important roles in defence response of host plants versus pathogens. While generation and detoxification of ROS is well understood, how varied ability of different isolates of pathogens to overcome host ROS, or ROS contribution to a particular isolate's pathogenicity, remains largely unexplored. Here, we report that transcriptional regulation of the ROS pathway, in combination with the insulin pathway, increases the pathogenicity of invasive species *Bursaphelenchus xylophilus*. The results showed a positive correlation between fecundity and pathogenicity of different nematode isolates. The virulent isolates from introduced populations in Japan, China and Europe had significantly higher fecundity than native avirulent isolates from the USA. Increased expression of *Mn-SOD* and reduced expression of *catalase/GPX-5* and H_2O_2 accumulation during invasion are associated with virulent strains. Additional H_2O_2 could improve fecundity of *Bu. xylophilus*. Furthermore, depletion of *Mn-SOD* decreased fecundity and virulence of *Bu. xylophilus*, while the insulin pathway is significantly affected. Thus, we propose that destructive pathogenicity of *Bu. xylophilus* to pines is partly owing to upregulated fecundity modulated by the insulin pathway in association with the ROS pathway and further enhanced by H_2O_2 oxidative stress. These findings provide a better understanding of pathogenic mechanisms in plant–pathogen interactions and adaptive evolution of invasive species.

This article is part of the theme issue 'Biotic signalling sheds light on smart pest management'.

1. Introduction

The pine wood nematode (PWN), *Bursaphelenchus xylophilus*, is a dangerous invasive species that causes pine wilt disease. In its native North American range, it causes little economic damage to native pine trees; however, it has devastating effects in the pine forests of Japan, China, Korea and Europe [1–4], and poses a serious threat to pine forests globally. Notably, a closely related sibling species *Bursaphelenchus mucronatus*, has a worldwide distribution but very low pathogenicity to pines in these regions [5,6].

At present, *Bu. xylophilus* has differentiated into avirulent (low pathogenicity) and virulent (high pathogenicity) isolates. The virulent isolates are spreading rapidly in new regions, especially in Europe and Northern China [7–9]. With a short generation time and a capacity for rapid evolution, invasive species have become a growing threat to ecosystems around the world [10,11]. Thus, there is an urgent need to characterize the molecular mechanisms of *Bu. xylophilus*'s destructive pathogenicity to pine trees.

During the early stages of most plant–pathogen interactions, a phenomenon known as oxidative burst often takes place at the site of attempted invasion [12–14]. These reactive oxygen species (ROS), which can be toxic to organisms, are detoxified rapidly by various cellular enzymatic mechanisms [8]. ROS, including superoxide anion ($O^{2-}\cdot$), hydrogen peroxide (H_2O_2) and hydroxyl radicals (OH), are considered to be very important in the interaction of pathogen and plant [15,16]. H_2O_2 was produced mainly by superoxide dismutase (*SOD*) and could be removed by *catalase* and various peroxidases, such as glutathione peroxidases (*GPX*) [17]. It could cross the plasma membrane and plays an important role in the host–pathogen interactions [18]. Genes such as *SOD*s, *catalase*, *GPX*s and cytochromes P450 (*CYP450*s) are linked to H_2O_2 homeostasis [19,20]. After a pathogen infects and colonizes host plants, mortality of the host is strongly correlated to the pathogen's fecundity [7,21,22]. Commonly, fecundity is determined by reproduction-related genes, like in nematodes belonging to the insulin and TGF-β signalling pathways [23]. Though it is reported that pathogens are able to stimulate ROS, particularly the generation of H_2O_2 [24], most studies are focused on ROS of host plants [13,14]. The contribution of ROS to the pathogenicity and fecundity of destructive pathogens remains largely unexplored.

In this study, we compared the pathogenicity of *Bu. xylophilus* isolates from different geographical regions to understand their potential to become virulent. We also identified variation in gene expression among different virulent isolates that were associated with the physiological processes of detoxification, development, reproduction, defence and pathogenicity. Our results revealed the upregulation of *Mn-SOD* in the ROS pathway and accumulation of H_2O_2 in virulent isolates during invasion could increase the pathogenicity of *Bu. xylophilus*. These findings help explain the molecular mechanisms behind PWN invasion and evolution of highly virulent isolates of *Bu. xylophilus*.

2. Material and methods

(a) Nematode isolates and culture condition

A total of 18 different isolates of nematodes were used in this study. Six isolates of *Bu. xylophilus* (CN-Bx1, CN-Bx2, CN-Bx3, CN-Bx4, CN-Bx5 and CN-Bx6) were obtained from Zhejiang, Jiangsu, Shaanxi (two isolates), Guangxi and Shandong province in China. The other isolates included three Japanese isolates (JP-Bx1, JP-Bx2 and JP-Bx3), two American (US) isolates (US-Bx1 and US-Bx2), and three European isolates (Eu-Bx1, Eu-Bx2 and EU-Bx3). All JP, CN and EU nematode isolates were collected from forests that experienced severe economic damage caused by *Bu. xylophilus*. An isolate of *Bu. mucronatus* (CN-Bm1), obtained from Zhejiang province, was used as a control. Three European *Bu. mucronatus* isolates (EU-Bm1, EU-Bm2 and EU-Bm3) were provided by the NemaLab-ICAM Department of Biologia, Universidade de Évora, Portugal.

The isolates were grown on cultivated *Botrytis cinerea* using potato dextrose agar (PDA) plates at 25°C for 10 days. The Baermann funnel method was used to separate *Bu. xylophilus* from PDA plates. *Bursaphelenchus xylophilus* was collected by centrifugation at 5000 *g* for 3 min and washed three times with distilled water. Approximately 2000 nematodes of each isolate were injected into 3-year-old black pine saplings in the field. After a period of two months, the pine saplings were cut, and nematodes were extracted from the pieces of cut wood using the Baermann funnel method [25]. The physical condition of pine saplings was analysed according to needle colour and orientation. Furthermore, each experiment required at least 30 pine saplings, which were injected by each nematode isolate from the field tests. Inbred lines of CN-Bx1 and US-Bx1 were used as experimental models [26].

(b) Nucleic acid extraction

Total DNA and RNA were extracted using the DNeasy or RNeasy Mini Kit (Qiagen, USA) according to the manufacturer's protocol. Samples were stored at −80°C. DNA and RNA concentrations were determined by a NanoDrop ND-2000 spectrophotometer (NanoDrop Products, USA). The quality of DNA was assessed by agarose gel electrophoresis. The integrity of RNA was verified on an Agilent 2100 BioAnalyzer (Agilent, USA).

(c) Assembly of transcriptome and identification of differentially expressed genes

The CN-Bx1 and US-Bx1, as representatives of virulent and avirulent isolates, were used for RNA sequencing. About 10 µg of total RNA was extracted from each sample using oligo (dT) magnetic bead-based enrichment technology (Invitrogen, USA). Next, paired-end RNA-seq libraries were prepared following Illumina's library construction protocol. The libraries were sequenced on an Illumina HiSeq 2000 platform (Illumina, USA) at the Beijing Institute of Genomics, Chinese Academy of Sciences. FASTQ files were produced and sorted for further analysis. Low-quality reads, microbial contaminations and adapter sequences were removed, and leftover clean reads were assembled *de novo* using Trinity [27]. All unigenes were annotated using a BLAST search against the non-redundant protein database (nr) and the Swiss-Prot database with a cut-off *E*-value $< 10^{-5}$. The R package RSEM was used to calculate the fragments per kilobase of exon per million fragments mapped (FPKM) value [28,29] and the differentially expressed genes (DEGs) were filtered out by R package DEGseq [30]. The genes were considered differentially or significantly expressed if they had value of $p < 0.05$ and a fold change of either greater than 2 (upregulated) or less than 0.5 (downregulated) [31].

(d) Quantitative real time-polymerase chain reaction analysis

The expression levels of the genes associated with detoxification, development, reproduction and parasitism were further analysed using quantitative real time-polymerase chain reaction (qRT-PCR). Three virulent isolates (JP-Bx3, CN-Bx1 and EU-Bx3) and two avirulent isolates (US-Bx1 and US-Bx2) were selected as representative strains with high and low fecundities, respectively. RNA was treated with DNaseI (Invitrogen) before cDNA synthesis. The cDNA was synthesized by Fast Quant RT Kit (Tiangen, China). The qRT-PCR was performed on a MX3005P system (Agilent Stratagene, USA) using SYBR® Premix Ex Taq™ (TaKaRa, Japan) according to the manufacturer's instructions. The qRT-PCR data were collected from software MXPro v 4.1 and exported to Microsoft Excel for analysis [32]. All experiments were done in triplicate and normalized relative to expression levels of the internal control gene encoding β-actin [33]. The primers used are indicated in the electronic supplementary material, table S2.

(e) Expression and purification of recombinant Mn-SOD protein

To amplify cDNA of *Mn-SOD*, PCR was performed using specific primers (electronic supplementary material, table S2). The PCR product was digested with restriction enzymes (BamHI and SalI) and cloned into pET-28a. The resulting recombinant plasmid was sequenced to confirm correct insertion. The expression, extraction and affinity purification *of Mn-SOD* was performed under non-denaturing conditions as previously described [34]. Briefly, soluble

protein of Mn-SOD was extracted from the culture medium and purified by Ni–NTA (nickel–nitrilotriacetic acid; Qiagen, Germany) agarose column. The affinity-purified Mn-SOD protein was subjected to sodium dodecyl sulphate-polyacrylamide gel electrophoresis (SDS-PAGE), immunoblot and peptide mass fingerprint analyses using nano-scale liquid chromatographic tandem mass spectrometry (nLC-MS/MS, Thermo Scientific, USA). The purified protein was stored at −80°C in Tris–HCl buffer (20 mM Tris, 150 mM NaCl and 1 mM DTT, pH 6.5). The activity of this protein was measured using the xanthine oxidase method [35]. A rabbit polyclonal antiserum was prepared against the recombinant Mn-SOD (BGI, China).

(f) Western blotting and immunohistochemistry

Western blot analysis was performed to measure the protein level of Mn-SOD in nematodes. Briefly, nematodes were homogenized in 100 µl of breaking buffer by vigorous shaking with a 3 mm steel ball as described previously [36]. Aliquots of protein samples were resolved on 4–15% gradient SDS–PAGE (Bio-Rad, USA) and electrotransferred to polyvinylidene difluoride membranes (Invitrogen, USA). After blocking, the membranes were incubated with the primary antibody and secondary anti-rabbit IgG (H + L) horseradish peroxidase conjugate (Promega, USA). Actin (I-19) (Santa Cruz Biotechnology, USA) was used as loading control. For immunohistochemistry analysis of Mn-SOD in US-Bx1, US-Bx2, JP-Bx3, CN-Bx1 and EU-Bx3, staining and visualization were performed as previously described [37]. Frozen sections were prepared by precise dissection under Leica CM1900 (Germany) following a 10 min incubation at 37°C and subsequent fixation in cold acetone. After blocking with 2% bovine serum albumin solution, the sections were simultaneously incubated with primary antibody and Alexa Fluor® 488 goat anti-rabbit IgG (Invitrogen, USA). 4′,6-diamidino-2-phenylindole (DAPI; Sigma-Aldrich, USA) was used as nuclear dye. The samples were analysed with a confocal microscope (Zeiss, Germany).

(g) Quantitative determination of hydrogen peroxide production in *Bursaphelenchus xylophilus*

Selected nematode isolates (US-Bx1, US-Bx2, JP-Bx3, CN-Bx1 and EU-Bx3) were used for the quantitative determination of H_2O_2 by Amplex® Red Hydrogen Peroxide Assay Kit (Invitrogen, USA). Collected nematodes were washed with PBST (phosphate buffered saline (PBS) containing 0.5% Tween 20, pH 7.2–7.4) and centrifuged. The collected nematodes and supernatant were retained for further measuring H_2O_2 content *in vivo* and *in vitro*. Protein concentrations of nematodes were determined using the Bradford assay (Bio-Rad, USA). All experiments were performed in three different sample sets (biological replicates) with two technical replicates per sample.

(h) *In vivo* functional analysis of hydrogen peroxide

To elucidate the *in vivo* function of H_2O_2 (Bx + H_2O_2), nematodes were soaked in a 20 mM solution of H_2O_2 (no nematode death in 8 h). Nematodes of selected isolates (US-Bx1, US-Bx2, JP-Bx3, CN-Bx1 and EU-Bx3) were used in each treatment. Approximately 2000 treated nematodes were injected into pine saplings. After two months, the physical condition of the pine saplings was evaluated by examining needle colour and orientation. Thirty pine saplings were used as a replicate study set for each treatment used in field tests. Meanwhile, under laboratory conditions, 200 treated nematodes of the five isolates were inoculated in *Bo. cinerea* culture plates. After 10 days, the nematodes were extracted using the Baermann funnel method and counted.

(i) *Mn-SOD* double stranded RNA synthesis

Double stranded RNA (dsRNA) synthesis was performed as previously described. Briefly, PCR was performed using the cDNA samples as templates to generate 400 bp *Mn-SOD* specific fragments using both sense and antisense primers (electronic supplementary material, table S2) fused with T7-phage promoter sequences. Synthesis of dsRNA was accomplished by simultaneous transcription of both strands of the template by the T7 RiboMAX™ Express RNAi System (Promega, USA). The nematodes were collected and washed by PBST buffer. For each reaction, around 2000 nematodes were soaked in dsRNA (final concentration 60 µg ml^{-1}) in a final volume of 50 µl. Control samples were soaked in dsRNA of green fluorescent protein (60 µg ml^{-1}). All the soaked samples were incubated in an orbital shaker at 180 rpm, 20°C for 24 h. After soaking, the nematodes were washed three times with double distilled water (ddH_2O).

(j) *In vivo* functional analysis of *Mn-SOD*

To elucidate the *in vivo* function of *Mn-SOD* (Bx + ds*Mn-SOD*), nematodes were soaked in a solution of *Mn-SOD* dsRNA (60 µg ml^{-1}). Around 2000 nematodes of selected isolates (US-Bx1, US-Bx2, JP-Bx3, CN-Bx1 and EU-Bx3) were used in each treatment. Treated nematodes were injected into pine saplings [38]. After two months, nematodes were recovered from the pine saplings using the Baermann funnel method. The physical condition of the pine saplings was evaluated by needle colour and orientation. Thirty pine saplings were used as a duplicate study set for each treatment used in field tests. Since the population of US isolates could not be found in the field in China, and laboratory simulation was tested as follows: approximately 200 nematodes of the five isolates supplemented with *Mn-SOD* dsRNA (60 µg ml^{-1}) and were inoculated in *Bo. cinerea* culture plates. After 15 days, the nematodes were extracted using the Baermann funnel method and counted.

(k) Relationship between *Mn-SOD* and fecundity genes

Following interference of *Mn-SOD* gene expression of the five isolates, the RNA of nematodes from each of the five isolates, with and without dsRNA, were extracted. The transcriptional levels of *Mn-SOD*, *daf-9*, *daf-12* and *daf-16* were analysed by qRT-PCR. This test was repeated with three experimental and two technical replications. Primers were used as indicated in the electronic supplementary material, table S2.

(l) Statistical analysis

In all experiments, the normality of data was measured using the Kolmogorov–Smirnov test, and homogeneity of group variances was screened using Levene's test. The statistical significance for each gene between the two groups was evaluated by the unpaired two-tailed Student's *t*-test or Mann–Whitney *U* test, depending on the results of the tests of normality and homogeneity. Data obtained from Levene's test were subject to one-way ANOVA with Tukey's test or Dunnett's T3 depending on the results of the tests of normality and homogeneity. The correlations between the mean nematode population size and mortality of host pines were tested with Pearson's correlation coefficient. Data were analysed by SPSS 18.0 software (SPSS, Inc., Chicago, USA). All quantitative data were represented as mean ± s.e.

3. Results

(a) Differences in fecundity, pathogenicity and transcriptome of *Bursaphelenchus xylophilus* isolates

To capture the variation in pathogenicity among different *Bu. xylophilus* populations, 18 isolates from the US, Japan, China and Europe were investigated. Pine saplings were inoculated with nematodes, and after two months nematode populations and mortality of host pine trees were analysed.

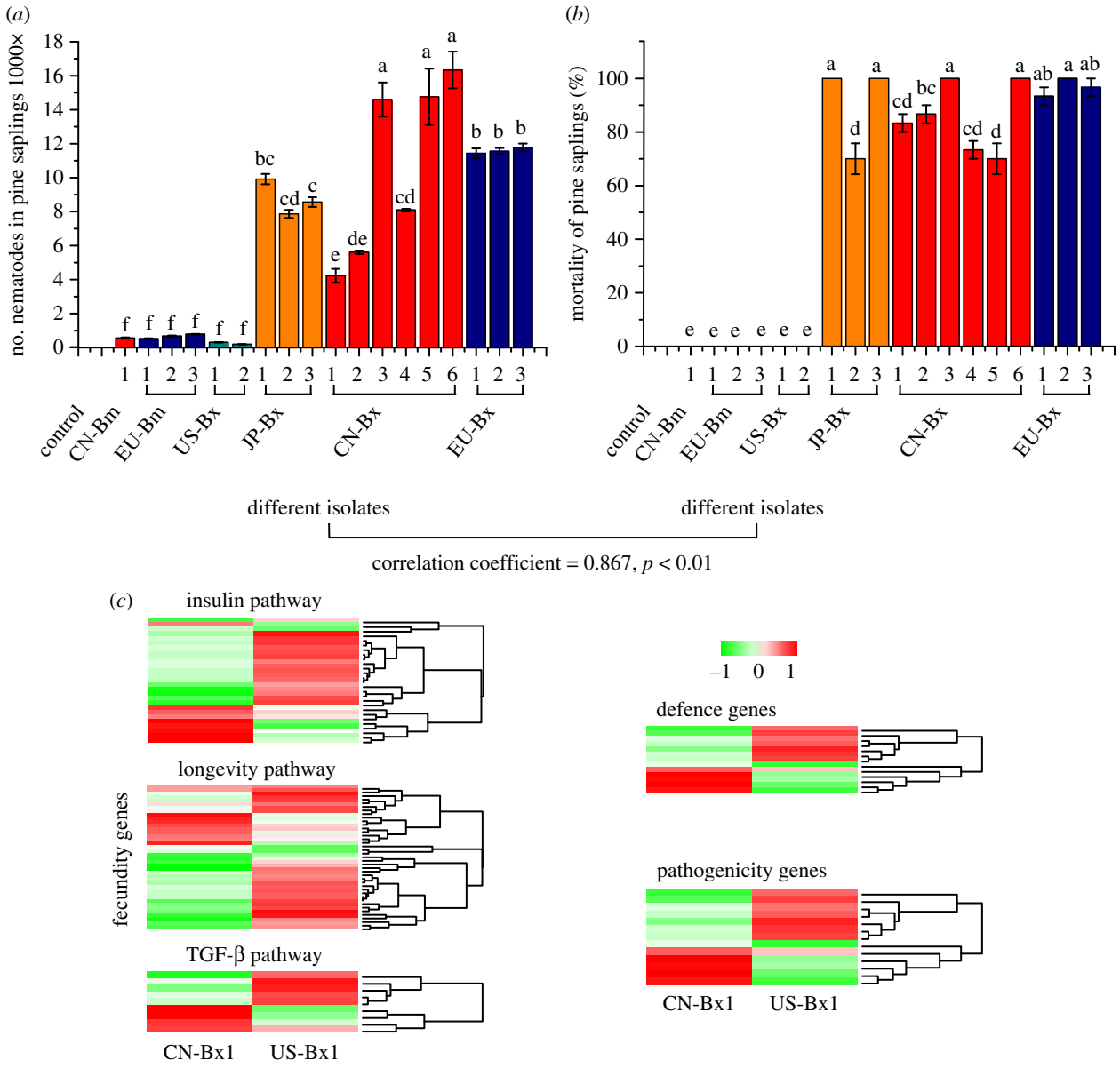

Figure 1. Comparative analysis of fecundity, pathogenicity and transcriptome of different nematodes isolates. (*a*) Fecundity of 18 isolates of nematodes in pine saplings. The different colour columns represent the following: cyan, US isolates (US-Bx1 and US-Bx2); orange, Japanese isolates (JP-Bx1, JP-Bx2 and JP-Bx3); red, Chinese isolates (CN-Bm1 (*Bu. mucronatus*), CN-Bx1, CN-Bx2, CN-Bx3, CN-Bx4, CN-Bx5 and CN-Bx6); blue, European isolates (EU-Bm1, EU-Bm2, EU-Bm3, EU-Bx1, EU-Bx2 and EU-Bx3) and the blank column represents the control. (*b*) Mortality of pine saplings infected by different nematode isolates. The physical condition of pine saplings was judged by the needle colour and orientation. Different letters indicate statistical differences in the mean. Error bars represents ±s.e. Bm (*Bu. mucronatus*) was an avirulent sibling species. (*c*) Functional classification of the selected genes in CN-Bx1 and US-Bx1 isolates and heatmap representing the DEGs of selected genes in CN-Bx1 and US-Bx1. The selected genes were associated with fecundity, defence and pathogenicity.

The results showed that nematode populations in pine saplings inoculated with JP-Bx, CN-Bx and EU-Bx isolates were five- to 80-fold higher compared with those of US-Bx and *Bu. mucronatus* isolates (figure 1*a*). There were no significant differences between nematode populations in pine saplings inoculated with US-Bx isolates and those with *Bu. mucronatus* (figure 1*a*). Saplings inoculated with avirulent isolates, *Bu. mucronatus* and US-Bx were healthy with green needles. However, the JP-Bx, CN-Bx and EU-Bx isolates were found to be pathogenic as these saplings inoculated with these isolates wilted and the needles yellowed significantly. The mortality of saplings ranged from 70% (JP-Bx2 and CN-Bx5) to 100% (JP-Bx1, JP-Bx3, CN-Bx3, CN-Bx6 and EU-Bx2), which was significantly higher than those inoculated with US-Bx and *Bu. mucronatus*. Thus, the pathogenicity of all the JP-Bx, CN-Bx and EU-Bx isolates was much higher compared with US-Bx isolates and *Bu. mucronatus* (figure 1*b*). Consequently, a tight positive correlation was observed between nematode population size and pathogenicity (figure 1*a*), with higher fecundity resulting in an elevated degree of pathogenicity and vice versa.

The transcriptional differences between the avirulent isolates (US-Bx) and virulent isolates (JP-Bx, CN-Bx and EU-Bx) were clearly shown in comparative transcriptome analysis of two representative isolates, virulent strain CN-Bx1 and avirulent strain US-Bx1. A total of 13 381 genes were annotated in the transcriptomes of CN-Bx1 and US-Bx1. We characterized 301 genes related to fecundity, defence and pathogenicity. Among them, 120 DEGs (electronic supplementary material, table S1) were distributed among the different functional categories. These genes were divided into three categorical groups including fecundity, defence and pathogenicity genes (figure 1*c*). Most fecundity genes belong to insulin, longevity

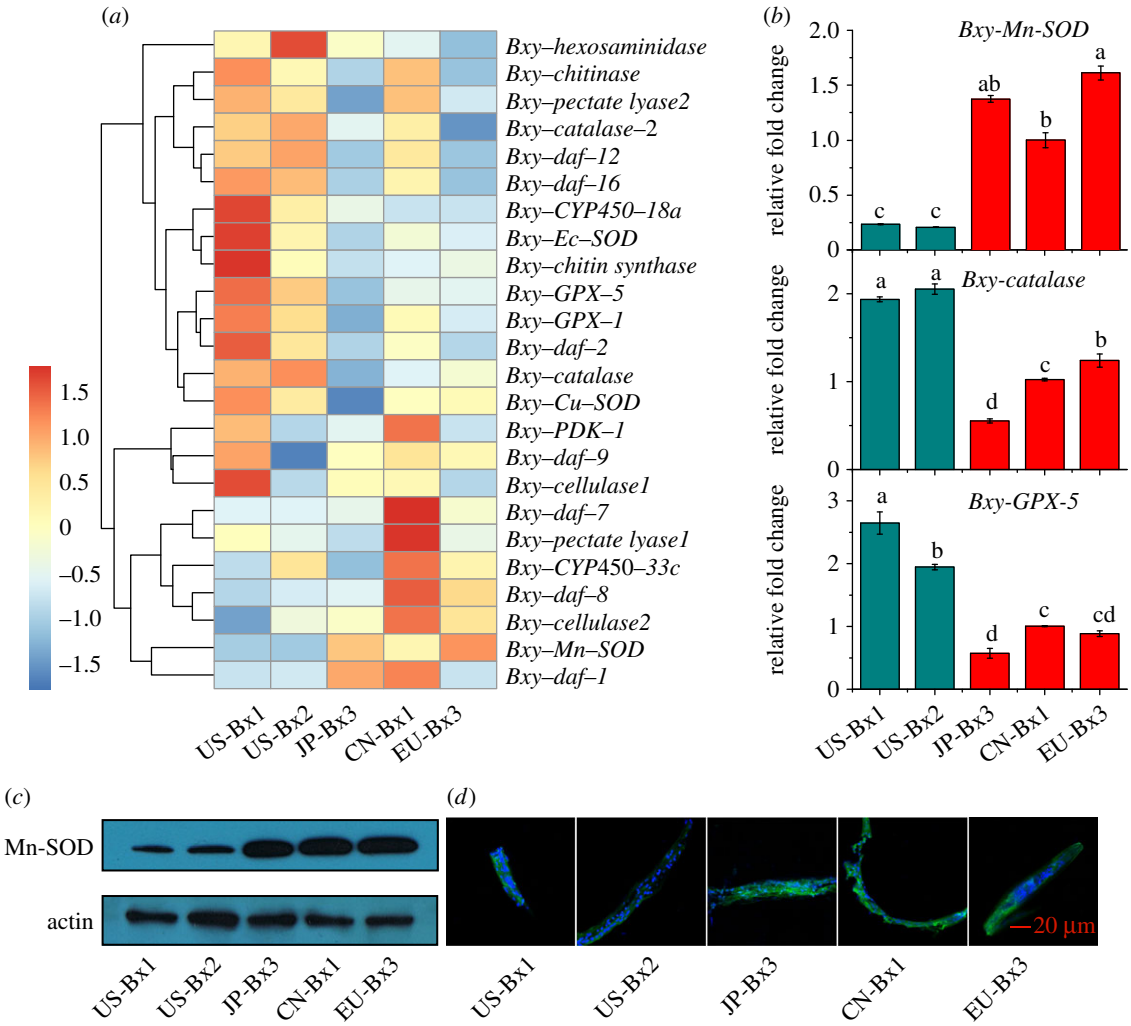

Figure 2. Expression analysis of the typical selected genes from different nematode isolates. (*a*) Heatmap showing the expression of characterized genes in US-Bx1, US-Bx2, JP-Bx3, CN-Bx1 and EU-Bx3 isolates using qRT-PCR. Selected genes are associated with defence, development, reproduction and pathogenicity. The genes *Bxy-catalase-1*, *Bxy-catalase-2*, *Bxy-GPX-1*, *Bxy-GPX-5*, *Bxy-CYP450-18a*, *Bxy-CYP450-33c*, *Bxy-Cu-SOD*, *Bxy-Ec-SOD* and *Bxy-Mn-SOD* are related to defence. The genes *Bxy-daf-2*, *Bxy-daf-12*, *Bxy-daf-16*, *Bxy-daf-1*, *Bxy-daf-7*, *Bxy-daf-8* and *Bxy-daf-9* are related to fecundity. *Bxy-chitin synthase*, *Bxy-chitinase* and *Bxy-hexosaminidase* are related to development. *Bxy-cellulase1*, *Bxy-cellulase2*, *Bxy-pectate lyase1* and *Bxy-pectate lyase2* are related to pathogenicity. (*b*) Expression of genes involved in the ROS pathway in US-Bx1, US-Bx2, JP-Bx3, CN-Bx1 and EU-Bx3 isolates. The data were derived from figure 2*a*. (*c*) Western blots showed that the protein level of Mn-SOD was higher in JP-Bx3, CN-Bx1 and EU-Bx3 isolates than that of US-Bx1 and US-Bx2 isolates. Actin was used as the loading control. (*d*) Images showing a higher accumulation of Mn-SOD protein in JP-Bx3, CN-Bx1 and EU-Bx3 isolates compared with that of US-Bx1 and US-Bx2 isolates, characterized by immunofluorescence. For immunofluorescence staining, Mn-SOD was stained with anti-rabbit IgG Alex Fluor® 488 (red). Nuclei were stained with DAPI dye (blue).

and TGF-β pathways. In the insulin and longevity pathways, the number of upregulated genes in CN-Bx1 was lower compared with the number of downregulated genes in US-Bx1 (figure 1*c*). Results showed that virulent CN-Bx1 had higher fecundity, supported by high nematode populations observed in pine saplings (figure 1*a*). However, there was no significant difference in the number of genes regulated among the TGF-β pathway, defence and pathogenicity genes between CN-Bx1 and US-Bx1. Interestingly, in the defence category, *Mn-SOD* and *Cu-SOD*, genes upstream of the ROS pathway were expressed higher in CN-Bx1 compared with US-Bx1. By contrast, *catalase*, a gene downstream of the ROS pathway, was expressed lower in CN-Bx1 compared with US-Bx1.

(b) Regulation variation of the reactive oxygen species pathway during invasion

To gain a better understanding of observed differences in our transcriptomic data, 24 genes related to fecundity, development, defence and pathogenicity were selected for qRT-PCR analysis to confirm the results from RNA-seq based analysis. Two US-Bx (US-Bx1 and US-Bx2) isolates were selected as avirulent representatives, and one JP-Bx (JP-Bx3), one CN-Bx (CN-Bx1) and one EU-Bx (EU-Bx3) isolates were selected as virulent representatives. Two genes in the insulin signalling pathway, *daf-16* and *daf-12* (fecundity suppressing genes), showed a lower expression level in virulent isolates (JP-Bx3, CN-Bx1 and EU-Bx3) in comparison with the avirulent isolates (US-Bx) (figure 2*a*). On the other hand, genes involved in the ROS pathway like *GPX-5* and *catalase* were expressed at least onefold lower, meanwhile *Mn-SOD* was expressed at least threefold higher in virulent isolates compared with avirulent isolates. This result clearly suggests the possible accumulation of H_2O_2 in the virulent nematodes. The expression of other assayed genes such as *daf-1*, *daf-7*, *daf-8*, *daf-2*, *Cu-SOD*, *Ec-SOD*, *gpx-1*, *cellulase1*, *cellulase2*, *pectate lyase1* and *pectate lyase2* did not show any consistent difference between virulent and avirulent isolates.

Using the same five isolates as mentioned above, we measured the protein levels of Mn-SOD via Western blots

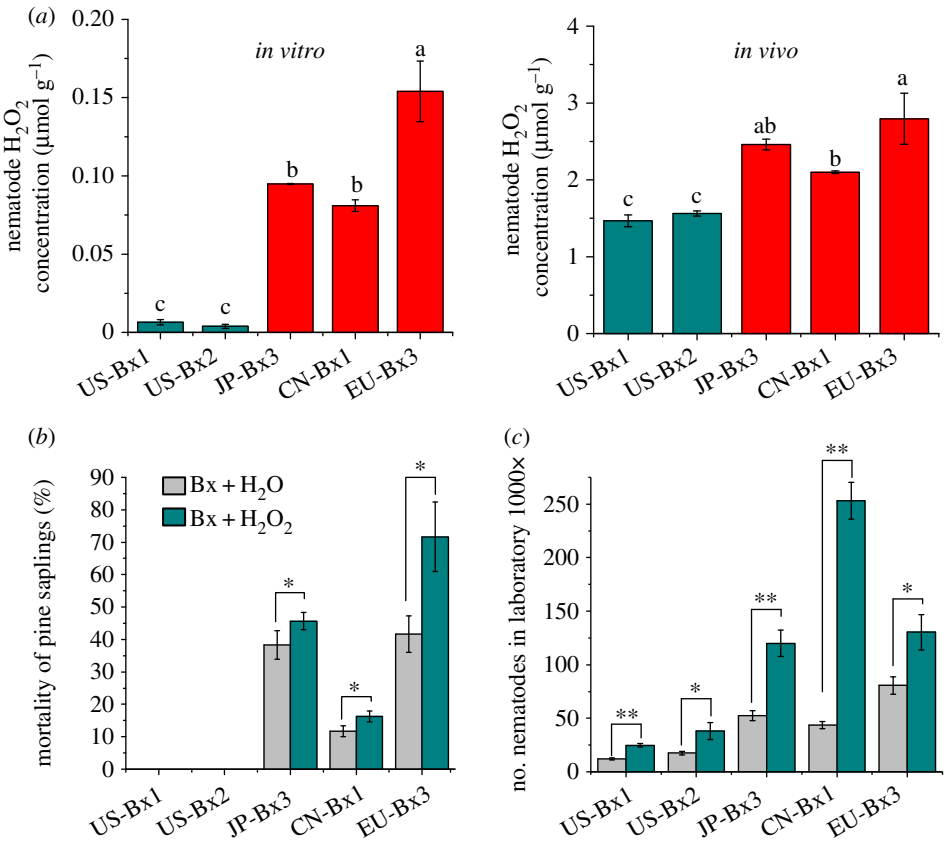

Figure 3. The role of H_2O_2 in pathogenicity of *Bu. xylophilus*. (*a*) The *in vitro* and *in vivo* H_2O_2 concentration of US-Bx1, US-Bx2, JP-Bx3, CN-Bx1 and EU-Bx3. Cyan columns represent isolates with lower fecundity rates (US-Bx1 and US-Bx2), whereas red columns represent isolates with higher fecundity rates (JP-Bx3, CN-Bx1 and EU-Bx3). Statistical differences in the mean are indicated with different letters. Error bars represent ± s.e. (*b*) Mortality of pine saplings infected with H_2O_2 (20 mM) treated US-Bx1, US-Bx2, JP-Bx3, CN-Bx1 and EU-Bx3 isolates. Physical condition was judged by the needle colour and orientation. Error bars represent ± s.e. (*c*) Fecundity of isolates US-Bx1, US-Bx2, JP-Bx3, CN-Bx1 and EU-Bx3 soaked in 20 mM H_2O_2 under laboratory conditions. *$p < 0.05$; **$p < 0.01$.

and immunofluorescence assays. Both experiments detected a high Mn-SOD protein content in virulent isolates (JP-Bx3, CN-Bx1 and EU-Bx3) (figure 2*c*,*d*). Although the candidate protein could be detected in avirulent nematodes (US-Bxs), it was much lower compared with virulent strains. These results not only confirmed that the high expression of *Mn-SOD* transcript in nematodes actually resulted in elevated protein levels, but also gave some indication about the underlying reason behind the avirulent nature of isolates. The low Mn-SOD protein levels in these nematodes might contribute to reduced fecundity, a hypothesis that has been further tested in subsequent experiments.

Phylogenetic analysis indicated that *Bu. xylophilus* Mn-SOD was clustered together with Mn-SODs from other nematodes forming a monophyletic group (electronic supplementary material, figure S1A). Mn-SOD recombinant protein was expressed and purified, followed by an enzymatic assay. Enzymatic activity of *Bu. xylophilus* Mn-SOD was calculated as 2696 U mg^{-1} by plotting a curve of inhibition rate versus concentration of protein (the inhibition rate of 50% corresponding to one unit of activity) (electronic supplementary material, figure S1B).

(c) Hydrogen peroxide promoted the pathogenicity and fecundity of *Bursaphelenchus xylophilus*

Next, we compared H_2O_2 accumulation in JP-Bx3, CN-Bx1 and EU-Bx3 isolates. During *in vitro* experiments, the H_2O_2 concentration was found to be higher in all three of the virulent isolates in comparison with avirulent isolates (figure 3*a*). The highest concentration occurred in EU-Bx3 (0.15 μmol g^{-1} protein). Similar differences in H_2O_2 concentration were also observed *in vivo* between virulent and avirulent isolates. The H_2O_2 concentration in virulent isolates (2.5 μmol g^{-1} protein on average) was higher than the avirulent isolates (1.5 μmol g^{-1} protein on average) (figure 3*a*) and positively correlated with the elevated expression of gene *Mn-SOD* as observed in qRT-PCR results. These experiments suggested that the genes in the ROS pathway might be responsible for the differences in pathogenicity observed between virulent (JP-Bx, CN-Bx and EU-Bx) and avirulent (US-Bx) nematode isolates.

To rigorously test the observed positive correlation between nematodes pathogenicity and H_2O_2 accumulation, field experiments were carried out. The pathogenicity of nematodes with enhanced H_2O_2 was higher, causing higher mortality of pine saplings, compared with nematodes without H_2O_2 enhancement. The EU-Bx3 with H_2O_2 was the most pathogenic isolate, causing 70% death of pine saplings. Avirulent isolates, US-Bx1 and US-Bx2, had no pathogenic effect on pines (figure 3*b*). Meanwhile, we tested the influence of H_2O_2 on nematode fecundity under laboratory conditions. The results showed that H_2O_2 (20 mM) could significantly improve the fecundity of *Bu. xylophilus* (figure 3*c*).

(d) *Mn-SOD* enhanced the fecundity of *Bursaphelenchus xylophilus*

To explore the function of *Mn-SOD* in nematode fecundity and its possible role in pine wilting, we introduced *Mn-SOD* dsRNA

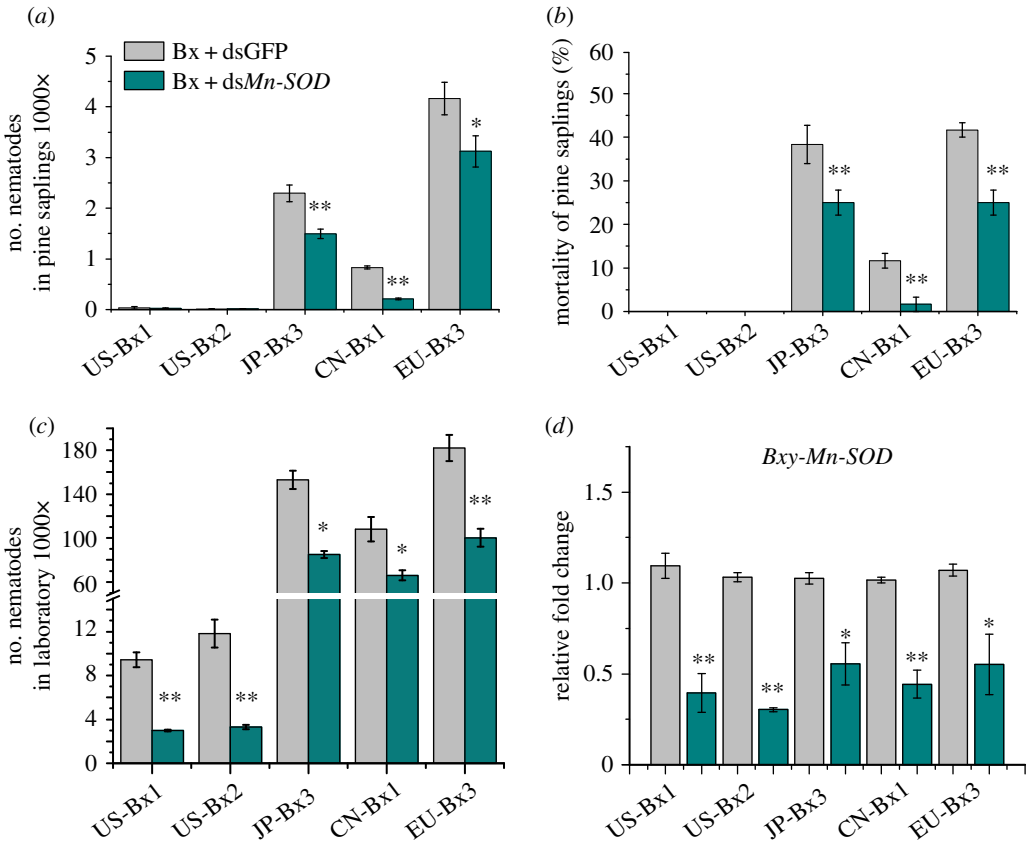

Figure 4. The role of *Mn-SOD* in fecundity and pathogenicity of *Bu. xylophilus*. (*a*) Fecundity of isolates US-Bx1, US-Bx2, JP-Bx3, CN-Bx1 and EU-Bx3 in pine saplings treated with *Mn-SOD* dsRNA or dsGFP. (*b*) Mortality of pine saplings infected with *Mn-SOD* dsRNA-treated US-Bx1, US-Bx2, JP-Bx3, CN-Bx1 and EU-Bx3 isolates. Physical condition was judged by the needle colour and orientation. Error bars represent $\pm$ s.e. (*c*) Fecundity of isolates US-Bx1, US-Bx2, JP-Bx3, CN-Bx1 and EU-Bx3 soaked in *Mn-SOD* dsRNA under laboratory conditions. (*d*) The gene expression levels of isolates US-Bx1, US-Bx2, JP-Bx3, CN-Bx1 and EU-Bx3 after interference of *Mn-SOD*. *$p < 0.05$; **$p < 0.01$.

(Bx + ds*Mn-SOD*) into the nematodes. *Mn-SOD* (upstream of the ROS pathway) was knocked down by more than 50% by *Mn-SOD* dsRNA interference in all the five nematode isolates (figure 4*d*). dsRNA-mediated knockdown of the *Mn-SOD* gene resulted in reduced fecundity in these isolates (up to two-fold in CN-Bx1). An expected reduction of mortality was observed in pine saplings infected with *Mn-SOD* dsRNA-treated nematodes (Bx + ds*Mn-SOD*) in comparison with controls (figure 4*a*,*b*). It suggested a clear role of *Mn-SOD* in regulating the fecundity of virulent nematodes, thus contributing to the diseased state of the pine hosts. Only a few nematodes of US-Bx1 and US-Bx2 could be detected in pine saplings, confirming their characteristically non-pathogenic nature. However, under laboratory conditions, a basal decline of fecundity was observed in ds*Mn-SOD* added nematode isolates (figure 4*c*). Taken together, our results clearly indicated the positive role of *Mn-SOD* in enhancing nematode fecundity and pathogenicity, and ultimately its capacity to cause severe pine wilt.

(e) *Mn-SOD* alters the expression of other genes related to fecundity

Finally, we used dsRNA interference of *Mn-SOD* to investigate the molecular mechanism of *Mn-SOD*-mediated enhancement of nematode fecundity. The genes *daf-12*, *daf-16* and *daf-9* of insulin signalling pathway are known to be involved in nematode reproductive processes. While *daf-9* promotes reproduction, *daf-12* and *daf-16* show negative correlations with fecundity (figure 5*b*) [23]. In our study, the expression of these genes were assayed in nematodes interfered by *Mn-SOD* dsRNA. A significant repression of *daf-9* was observed in *Mn-SOD*-depleted nematodes while *daf-12* and *daf-16* were activated (figure 5*a*). These observations provide further evidence supporting our hypothesis of the role of *Mn-SOD* in regulating reproductive fecundity and furthering the potential for pathogenic invasion.

4. Discussion

Although numerous research has reported differences in gene expression during pathogen invasion [39,40], the molecular mechanism responsible for increased fecundity and pathogenicity has not been established. In this study, we found that upregulation of *Bu. xylophilus Mn-SOD* and downregulation of *catalase/GPX* increased the level of H_2O_2, resulting in a boost of fecundity and pathogenicity. Upregulation of *Mn-SOD* could suppress the insulin signalling pathway, which led to higher fecundity leading to further enhancement of pathogenicity promoting *Bu. xylophilus* invasion. *Bursaphelenchus xylophilus* reproduces quickly and the entire life cycle from fertilization to mature adult can be completed in 5 days in controlled laboratory conditions [41]. With a short reproductive cycle, *Bu. xylophilus* has the potential to evolve rapidly and acquire traits that aids its fecundity and pathogenicity. When *Bu. xylophilus* enters a new geographical niche, it will eventually evolve into a virulent or avirulent strain [7]. We speculate that the virulent strains will have the capability to adapt and multiply in the new environment [42] owing to

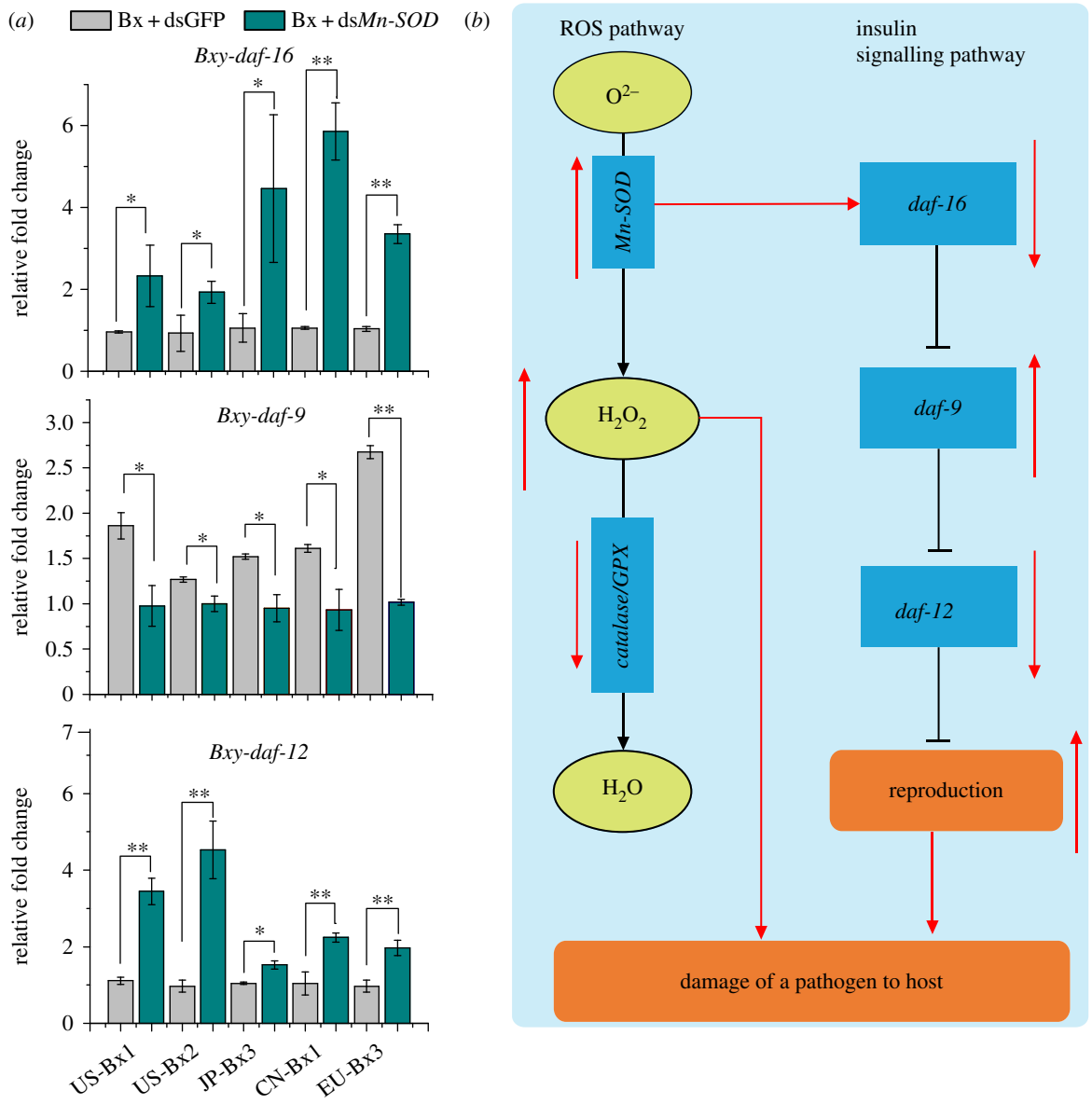

Figure 5. *Mn-SOD* regulates the expression of fecundity genes in nematodes. (*a*) qRT-PCR of nematode fecundity genes after *Mn-SOD* interference. The fecundity genes were *daf-16*/FOXO, *daf-9*/CYP450 and *daf-12*/nuclear hormone receptor (NHR). The grey columns (Bx + H_2O) represent the nematodes soaked in dsGFP as a control, while the cyan columns (Bx + *Mn-SOD* dsRNA) represent nematodes soaked in *Mn-SOD* dsRNA. Final concentration of *Mn-SOD* dsRNA used: 60 μg ml^{-1}. Error bars represent ± s.e. *$p < 0.05$; **$p < 0.01$. (*b*) Diagram showing the relationship between the insulin signalling pathway and the ROS pathway. Black arrows represent induction, while the terminated black lines represent suppression. Red arrows were our results.

expression of invasion-related genes like *Mn-SOD* and *catalase* which enhance its pathogenicity.

Most research on the ROS pathway is focused on its function in the oxidative burst and defence of the host plant [43]. However, the activation of the ROS pathway in the pathogens and its role in pathogenicity has not been clearly defined. We detected that the concentration of H_2O_2 in different *Bu. xylophilus* isolates was higher in virulent isolates (JP, CN and EU) compared with avirulent isolates (US), which could promote the pathogenicity and fecundity of *Bu. xylophilus*.

Most studies about the genetic basis of fecundity were focused on insulin signalling pathway elements, such as *daf-9*, *daf-12* and *daf-16* genes, which can further regulate the downstream gene *Mn-SOD* [44,45]. Our results showed that *Mn-SOD* expression changes could affect the upstream fecundity genes of *Bu. xylophilus*. Depletion of *Mn-SOD* in nematodes led to reproductive decline and downregulation of the reproduction-related gene *daf-9* and upregulation of reproduction repressed genes *daf-12* and *daf-16*. This function of *Bu. xylophilus Mn-SOD* is similar to a wasp's *Mn-SOD*, which showed a significant positive correlation between Mn-*SOD* and fecundity [46]. We reported that *Mn-SOD* could promote the fecundity and pathogenicity of *Bu. xylophilus* and downregulate its insulin signalling pathway, which is known to suppress its fecundity.

Taken together, our data demonstrate various genotypic differences between the virulent and avirulent isolates of *Bu. xylophilus*. An increase in the transcript level of *Mn-SOD* was observed in the virulent isolates during the invasion process. *Mn-SOD* enhanced the fecundity of nematodes by regulating genes related to fecundity, leading to the establishment of populations of pathogenic *Bu. xylophilus* in pine saplings. Our findings indicate a possible genetic mechanism behind the increased fecundity of *Bu. xylophilus* and the evolution of pathogenic strains. This deeper understanding facilitates the development of new approaches, such as using RNA interference to target expression of fecundity-related genes, to effectively control pine wilt disease globally.

Ethics. This study was carried out in full compliance with the laws of China. No specific permits were required for experiments involving *Bursaphelenchus* nematodes.

Data accessibility. The datasets supporting this article have been uploaded as part of the electronic supplementary material.

Authors' contributions. J.S., Z.Z. and L.Z. designed the study. W.Z. and L.Z. performed and analysed the biological experiments. J.Z. and Z.L. performed the immunofluorescence. H.Y. and Y.L. analysed the transcriptome of PWN. C.Z. sequenced the *Mn-SOD* gene. J.S., Z.Z. and W.Z. wrote the manuscript.

Competing interests. We have no competing interests.

Funding. This work was supported by the Chinese Academy of Sciences Strategic R&D Program (XDB11050000 and XDB11030600), the National Natural Science Foundation of China (NSFC 31630013, 31272323 and 31872298) and the High Technology Research and Development Program (HTRDP) of China (863 plan: 2014AA020529).

References

1. Nickle W, Golden A, Mamiya Y, Wergin W. 1981 On the taxonomy and morphology of the pine wood nematode, *Bursaphelenchus xylophilus* (Steiner &Buhrer 1934) Nickle 1970. *J. Nematol.* **13**, 385.
2. Cheng H, Lin M, Li W, Fang Z. 1983 The occurrence of a pine wilting disease caused by a nematode found in Nanjing. *Forest Pest. Dis.* **4**, 1–5.
3. Mota MM, Braasch H, Bravo MA, Penas AC, Burgermeister W, Metge K, Sousa E. 1999 First report of *Bursaphelenchus xylophilus* in Portugal and in Europe. *Nematology* **1**, 727–734. (doi:10.1163/156854199508757)
4. Yi CK, Byun BH, Park JD, Yang S, Chang KH. 1989 First finding of the pine wood nematode, *Bursaphelenchus xylophilus* (Steiner et Buhrer) Nickle and its insect vector in Korea. *Res. Rep. Forest. Res. Inst.* **38**, 141–149.
5. Cheng XY, Xie PZ, Cheng FX, Xu RM, Xie BY. 2009 Competitive displacement of the native species *Bursaphelenchus mucronatus* by an alien species *Bursaphelenchus xylophilus* (Nematoda: Aphelenchida: Aphelenchoididae): a case of successful invasion. *Biol. Invasions* **11**, 205–213. (doi:10.1007/s10530-008-9225-2)
6. Mamiya Y, Enda N. 1979 *Bursaphelenchus mucronatus* n. sp. (Nematoda: Aphelenchoididae) from pine wood and its biology and pathogenicity to pine trees. *Nematologica* **25**, 353–361. (doi:10.1163/187529279X00091)
7. Aikawa T, Kikuchi T. 2007 Estimation of virulence of *Bursaphelenchus xylophilus* (Nematoda: Aphelenchoididae) based on its reproductive ability. *Nematology* **9**, 371–377. (doi:10.1163/156854107781352007)
8. Li Z, Zhang Q, Zhou X. 2016 A 2-Cys peroxiredoxin in response to oxidative stress in the pine wood nematode, *Bursaphelenchus xylophilus*. *Sci. Rep.* **6**, 27438. (doi:10.1038/srep27438)
9. Zhao L *et al.* 2016 Ascarosides coordinate the dispersal of a plant-parasitic nematode with the metamorphosis of its vector beetle. *Nat. Commun.* **7**, 12341. (doi:10.1038/ncomms12341)
10. Colautti RI, Lau JA. 2015 Contemporary evolution during invasion: evidence for differentiation, natural selection, and local adaptation. *Mol. Ecol.* **24**, 1999–2017. (doi:10.1111/mec.13162)
11. Tayeh A, Hufbauer RA, Estoup A, Ravigne V, Frachon L, Facon B. 2015 Biological invasion and biological control select for different life histories. *Nat. Commun.* **6**, 5. (doi:10.1038/ncomms8268)
12. Alvarez ME, Lamb C. 1997 Oxidative burst-mediated defense responses in plant disease resistance. *Cold Spring Harbor Monogr. Archive* **34**, 815–839.
13. D'Autreaux B, Toledano MB. 2007 ROS as signalling molecules: mechanisms that generate specificity in ROS homeostasis. *Nat. Rev. Mol. Cell Biol.* **8**, 813–824. (doi:10.1038/nrm2256)
14. Quan LJ, Zhang B, Shi WW, Li HY. 2008 Hydrogen peroxide in plants: a versatile molecule of the reactive oxygen species network. *J. Integr. Plant. Biol.* **50**, 2–18. (doi:10.1111/j.1744-7909.2007.00599.x)
15. Lamb C, Dixon RA. 1997 The oxidative burst in plant disease resistance. *Annu. Rev. Plant Physiol. Plant Mol. Biol.* **48**, 251–275. (doi:10.1146/annurev.arplant.48.1.251)
16. Santos CS, Pinheiro M, Silva AI, Egas C, Vasconcelos MW. 2012 Searching for resistance genes to *Bursaphelenchus xylophilus* using high throughput screening. *BMC Genomics* **13**, 599. (doi:10.1186/1471-2164-13-599)
17. Henkle-Duhrsen K, Kampkotter A. 2001 Antioxidant enzyme families in parasitic nematodes. *Mol. Biochem. Parasitol.* **114**, 129–142. (doi:10.1016/S0166-6851(01)00252-3)
18. Levine A, Tenhaken R, Dixon R, Lamb C. 1994 H_2O_2 from the oxidative burst orchestrates the plant hypersensitive disease resistance response. *Cell* **79**, 583–593. (doi:10.1016/0092-8674(94)90544-4)
19. Strode C *et al.* 2008 Genomic analysis of detoxification genes in the mosquito *Aedes aegypti*. *Insect. Biochem. Mol. Biol.* **38**, 113–123. (doi:10.1016/j.ibmb.2007.09.007)
20. Jenney FE, Verhagen MF, Cui X, Adams MW. 1999 Anaerobic microbes: oxygen detoxification without superoxide dismutase. *Science* **286**, 306–309. (doi:10.1038/nbt.1883)
21. Wang Y, Yamada T, Sakaue D, Suzuki K. 2005 Variations in life history parameters and their influence on rate of population increase of different pathogenic isolates of the pine wood nematode, *Bursaphelenchus xylophilus*. *Nematology* **7**, 459–467. (doi:10.1163/156854105774355545)
22. Mitchell JE. 1979 The dynamics of the inoculum potential of populations of soil-borne plant pathogens in the soil ecosystem. In *Soil-borne plant pathogens* (eds B Schippers, W Gams), pp. 3–20. London, UK: Academic Press.
23. Fielenbach N, Antebi A. 2008 *C. elegans* dauer formation and the molecular basis of plasticity. *Genes Dev.* **22**, 2149–2165. (doi:10.1101/gad.1701508)
24. Hassani M, Salami SA, Nasiri J, Abdollahi H, Ghahremani Z. 2016 Phylogenetic analysis of PR genes in some pome fruit species with the emphasis on transcriptional analysis and ROS response under *Erwinia amylovora* inoculation in apple. *Genetica* **144**, 9–22. (doi:10.1007/s10709-015-9874-x)
25. Son JA, Moon YS. 2013 Efficiency of the Baermann funnel technique as revealed by direct counts of pine wood nematodes in pine tissue. *Nematology* **15**, 125–127. (doi:10.1163/15685411-00002690)
26. Zhang W, Zhang S, Kong X, Zhao LL. 2014 Inbreeding and reproductive comparison of *Bursaphelenchus xylophilus*. *Acta Ecol. Sin.* **34**, 3932–3936.
27. Grabherr MG *et al.* 2011 Full-length transcriptome assembly from RNA-Seq data without a reference genome. *Nat. Biotechnol.* **29**, 644–652. (doi:10.1038/nbt.1883)
28. Li B, Dewey CN. 2011 RSEM: accurate transcript quantification from RNA-Seq data with or without a reference genome. *BMC Bioinf.* **12**, 323. (doi:10.1186/1471-2105-12-323)
29. Tu Q, Cameron RA, Worley KC, Gibbs RA, Davidson EH. 2012 Gene structure in the sea urchin *Strongylocentrotus purpuratus* based on transcriptome analysis. *Genome Res.* **22**, 2079–2087. (doi:10.1101/gr.139170.112)
30. Wang L, Feng Z, Wang X, Wang X, Zhang X. 2010 DEGseq: an R package for identifying differentially expressed genes from RNA-seq data. *Bioinformatics* **26**, 136–138. (doi:10.1093/bioinformatics/btp612)
31. Xiong GH, Xing LS, Lin Z, Saha TT, Wang C, Jiang H, Zou Z. 2015 High throughput profiling of the cotton bollworm *Helicoverpa armigera* immunotranscriptome during the fungal and bacterial infections. *BMC Genomics* **16**, 321. (doi:10.1186/s12864-015-1509-1)
32. Hou Y, Wang XL, Saha TT, Roy S, Zhao B, Raikhel AS, Zou Z. 2015 Temporal coordination of carbohydrate metabolism during mosquito reproduction. *PLoS Genet.* **11**, e1005309. (doi:10.1371/journal.pgen.1005309)
33. Link CD, Taft A, Kapulkin V, Duke K, Kim S, Fei Q, Wood DE, Sahagan BG. 2003 Gene expression analysis in a transgenic *Caenorhabditis elegans* Alzheimer's disease model. *Neurobiol. Aging* **24**, 397–413. (doi:10.1016/S0197-4580(02)00224-5)
34. Jiang H, Wang Y, Ma C, Kanost MR. 1997 Subunit composition of pro-phenol oxidase from *Manduca sexta*: molecular cloning of subunit proPO-p1. *Insect.*

Biochem. Mol. Biol. **27**, 835–850. (doi:10.1016/S0965-1748(97)00066-0)

35. Sun WH, Liu F, Chen Y, Zhu YC. 2012 Hydrogen sulfide decreases the levels of ROS by inhibiting mitochondrial complex IV and increasing SOD activities in cardiomyocytes under ischemia/reperfusion. *Biochem. Biophys. Res. Commun.* **421**, 164–169. (doi:10.1016/j.bbrc.2012.03.121)
36. Ainsworth EA, Gillespie KM. 2007 Estimation of total phenolic content and other oxidation substrates in plant tissues using Folin-Ciocalteu reagent. *Nat. Protoc.* **2**, 875–877. (doi:10.1038/nprot.2007.102)
37. Wang YH, Hu Y, Xing LS, Jiang H, Hu SN, Raikhel AS, Zou Z. 2015 A critical role for CLSP2 in the modulation of antifungal immune response in mosquitoes. *PLoS Pathog.* **11**, e1004931. (doi:10.1371/journal.ppat.1004931)
38. Xu XL, Wu XQ, Ye JR, Huang L. 2015 Molecular characterization and functional analysis of three pathogenesis-related cytochrome P450 genes from *Bursaphelenchus xylophilus* (Tylenchida: Aphelenchoidoidea). *Int. J. Mol. Sci.* **16**, 5216–5234. (doi:10.3390/ijms16035216)
39. Nasser W *et al*. 2014 Evolutionary pathway to increased virulence and epidemic group A *Streptococcus* disease derived from 3,615 genome sequences. *Proc. Natl Acad. Sci. USA* **111**, E1768–E1776. (doi:10.1073/pnas.1403138111)
40. Hodgins KA, Lai Z, Nurkowski K, Huang J, Rieseberg LH. 2013 The molecular basis of invasiveness: differences in gene expression of native and introduced common ragweed (*Ambrosia artemisiifolia*) in stressful and benign environments. *Mol. Ecol.* **22**, 2496–2510. (doi:10.1111/mec.12179)
41. Zhao BG, Futai K, Sutherland JR, Takeuchi Y. 2008 *Pine wilt disease*. Berlin, Germany: Springer.
42. Kiyohara T, Bolla R. 1990 Pathogenic variability among populations of the pinewood nematode, *Bursaphelenchus xylophilus*. *For. Sci.* **36**, 1061–1076.
43. Mengiste T. 2012 Plant immunity to necrotrophs. *Annu. Rev. Phytopathol.* **50**, 267–294. (doi:10.1146/annurev-phyto-081211-172955)
44. Kaletsky R, Lakhina V, Arey R, Williams A, Landis J, Ashraf J, Murphy CT. 2016 The *C. elegans* adult neuronal IIS/FOXO transcriptome reveals adult phenotype regulators. *Nature* **529**, 92–96. (doi:10.1038/nature16483)
45. Essers MA, de Vries-Smits LM, Barker N, Polderman PE, Burgering BM, Korswagen HC. 2005 Functional interaction between beta-catenin and FOXO in oxidative stress signaling. *Science* **308**, 1181–1184. (doi:10.1126/science.1109083)
46. Büyükgüzel K. 2006 Malathion-induced oxidative stress in a parasitoid wasp: effect on adult emergence, longevity, fecundity, and oxidative and antioxidative response of *Pimpla turionellae* (Hymenoptera: Ichneumonidae). *J. Econ. Entomol.* **99**, 1225–1234. (doi:10.1093/jee/99.4.1225)